Biological ramifications of climate-change-mediated oceanic multi-stressors

Philip W. Boyd[1]*, Sinikka T. Lennartz[2,3], David M. Glover[4] and Scott C. Doney[4]

Climate change is altering oceanic conditions in a complex manner, and the concurrent amendment of multiple properties will modify environmental stress for primary producers. So far, global modelling studies have focused largely on how alteration of individual properties will affect marine life. Here, we use global modelling simulations in conjunction with rotated factor analysis to express model projections in terms of regional trends in concomitant changes to biologically influential multi-stressors. Factor analysis demonstrates that regionally distinct patterns of complex oceanic change are evident globally. Preliminary regional assessments using published evidence of phytoplankton responses to complex change reveal a wide range of future responses to interactive multi-stressors with <20–300% shifts in phytoplankton physiological rates, and many unexplored potential interactions. In a future ocean, provinces will encounter different permutations of change that will probably alter the dominance of key phytoplankton groups and modify regional productivity, ecosystem structure and biogeochemistry. Consideration of regionally distinct multi-stressor patterns can help guide laboratory and field studies as well as the interpretation of interactive multi-stressors in global models.

Multiple lines of evidence, ranging from time-series observations to climate modelling experiments, demonstrate the ongoing role of climate change in modifying many ocean properties such as temperature, salinity and pH (refs 1–3). Coupled ocean–atmosphere–land Earth system models link present-day evidence of a changing ocean[3] with that of a future ocean by providing detailed projections of how climate change will continue to alter concurrently a range of characteristics, for example, enhanced vertical density stratification in the upper ocean, over the coming decades[4]. The effect of changing conditions on marine life has been explored in detail using manipulation experiments in which individual oceanic properties such as pH are perturbed on the basis of future climate change modelling projections[5]. Initial global modelling studies concentrated on the potential impact of a subset of processes on planktonic organisms, for example, changes in temperature, nutrients and stratification on phytoplankton growth[4] or ocean acidification on calcification[6]. Recently, coupled Earth system model studies have begun to focus more on the complexity of these climate-change-mediated environmental changes, including the overlapping effects of warming, acidification and/or hypoxia and their influence on ocean biogeochemistry[2,7]. The goal of our study is a new framework for interpreting and visualizing coupled Earth system model results and helping design future laboratory and field experiments.

Two complementary approaches have been taken by modellers investigating how changing oceanic conditions will alter phytoplankton productivity and the resulting biogeochemical signatures[8,9]. A number of coupled Earth models incorporate phytoplankton–zooplankton dynamics by representing either a single generic phytoplankton or several phytoplankton functional groups[7,8] (for example, size classes, biominerals). At the other end of the spectrum are simulations that use a phytoplankton community of ~100 'species' and allow for emergent behaviour[9]. Despite these previous advances in addressing the complex nature

of plankton communities, neither modelling approach (which includes our model, see later), as of yet, resolves the full complexity of phytoplankton physiological responses to multiple co-varying stressors evident from the rapid recent advances in laboratory and field manipulation studies[10,11].

A growing body of evidence from time-series observations[12] and manipulation experiments[10,11] reveals that biota such as phytoplankton will be significantly influenced by such concurrent and complex change, termed here oceanic multi-stressors. The effects of multi-stressors can be demarcated into independent and interactive (synergistic or antagonistic)[11,13]. The former are where individual stressors each alter phytoplankton physiology but do not interact, whereas in the latter case, the interplay between multi-stressors results in amplification or diminution of phytoplankton processes relative to the combined effects of the individual stressors alone. Laboratory and field studies have shown up to fourfold physiological amplification due to the interplay of multi-stressors, such as iron and temperature on polar diatoms[14]. Hence, there is a need for models to move beyond their reliance on simple and numerically rigid representations in contrast to the complexity and sensitivity suggested in laboratory multi-stressor studies. Models must further incorporate this widespread interactive facet of multi-stressors to investigate to what extent cumulative environmental stress may be exerted on oceanic biota.

Although coupled Earth system model experiments have been pivotal to better understanding the ramifications of climate change on the ocean, this rich source of information has been under-used so far as the basis for designing targeted process studies. Model projection results for different climate scenarios are often displayed as two-dimensional global maps of the change for each ocean property. Although qualitatively valuable for visualizing large-scale patterns (Fig. 1), these maps are usually considered in isolation from maps of trends in other oceanic properties[4]. Innovative visualization methods have been recently proposed for mapping simultaneously potential hotspots, such as the equatorial Pacific, where specific

[1]Institute for Marine and Antarctic Studies, University of Tasmania, Hobart, Tasmania 7005, Australia. [2]Institute for Geoecology, TU Braunschweig, 38106 Braunschweig, Germany. [3]Geomar, Helmholtz-Center for Oceanographic Research, 24105 Kiel, Germany. [4]Department of Marine Chemistry and Geochemistry, Woods Hole Oceanographic Institution, Woods Hole, Massachusetts 02543, USA. *e-mail: Philip.boyd@utas.edu.au
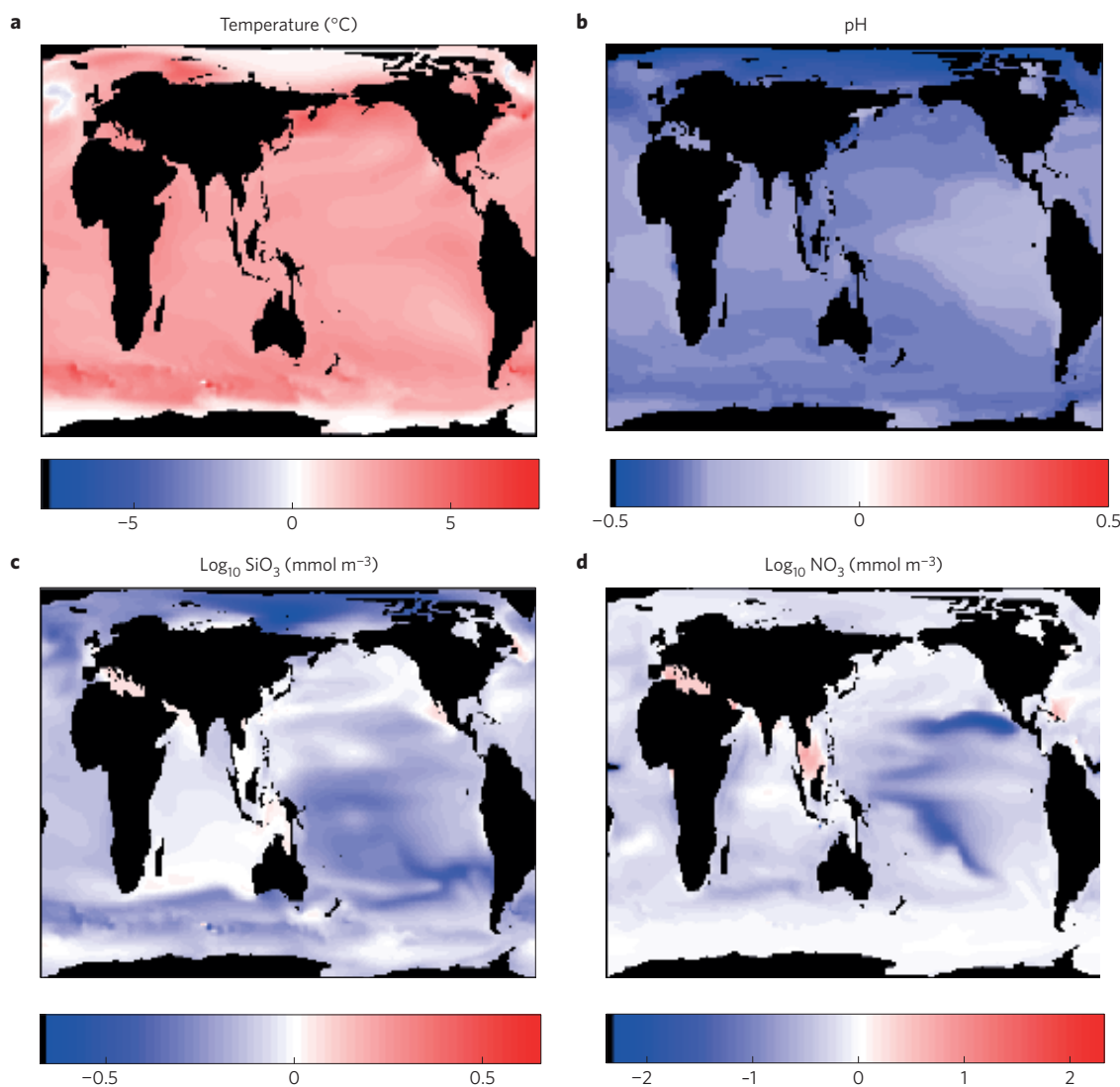
Figure 1 | Global maps of the change in four illustrative ocean properties between the decades (mean of 2081–2100) minus present (mean 1981–2000) from the CESM1(BEC) model simulations. a, Temperature (°C). **b**, pH. **c**, Log_{10} SiO_3 (mmol m^{-3}). **d**, Log_{10} NO_3 (mmol m^{-3}).

Table 1 | Summary of the statistical analysis for the global trends reported in Fig. 1.

	Temp. (°C)	Salinity (psu)	Ice fraction –	Log_{10} MLD (cm)	PAR (W m^{-2})	Windstress (dyn cm^{-2})	Pot. density (kg m^{-3})	Log_{10} SiO_3 (mmol m^{-3})	Log_{10} PO_4 (mmol m^{-3})	Log_{10} Fe (mmol m^{-3})	Log_{10} NO_3 (mmol m^{-3})	Alkalinity (meq m^{-3})	CO_3^{2-} (μmol kg^{-1})	pH –	p_{CO_2} (ppmv)
Global mean	2.5	−0.1	−0.03	−0.02	0.43	0.00	−0.73	−0.13	−0.31	0.07	−0.25	−6.52	−82.5	−0.32	486.8
Global s.d.	0.7	0.4	0.08	0.05	2.43	0.10	0.23	0.10	0.21	0.09	0.28	3.46	18.3	0.02	23.0
Global s.d. (province means)	0.45	0.24	0.06	0.02	1.47	0.06	0.22	0.05	0.15	0.05	0.15	2.59	14.71	0.01	15.76
Ratio s.d. (province mean/full grid)	0.70	0.61	0.77	0.40	0.61	0.60	0.70	0.51	0.69	0.50	0.55	0.75	0.80	0.76	0.69
Coef. of variation	0.3	3.9	2.69	2.54	5.67	154.3	0.31	0.78	0.68	1.38	1.11	0.53	0.22	0.07	0.05
Correl. temp.	1	0.5	0.42	0.39	−0.25	−0.16	−0.02	0.22	−0.20	0.18	−0.07	0.09	−0.15	0.30	0.20
Correl. p_{CO_2}	0.2	−0.1	−0.05	0.18	0.04	−0.14	−0.23	−0.22	−0.34	0.16	−0.07	−0.36	−0.28	−0.58	1

The table presents the global mean anomaly (difference between 2081–2100 and 1981–2000), the corresponding standard deviation, the global standard deviation of the province means, the ratio of standard deviations (province means/global means), the coefficient of variation (standard deviation divided by mean anomaly) and in addition the spatial correlation of variables with temperature and partial CO_2 pressure (p_{CO_2}). PAR denotes the average photosynthetically available radiation for the surface layer (10 m in the case of the CESM1(BEC)) averaged over 24 h for each month[16,42]. MLD: mixed-layer depth; PAR: photosynthetically available radiation.
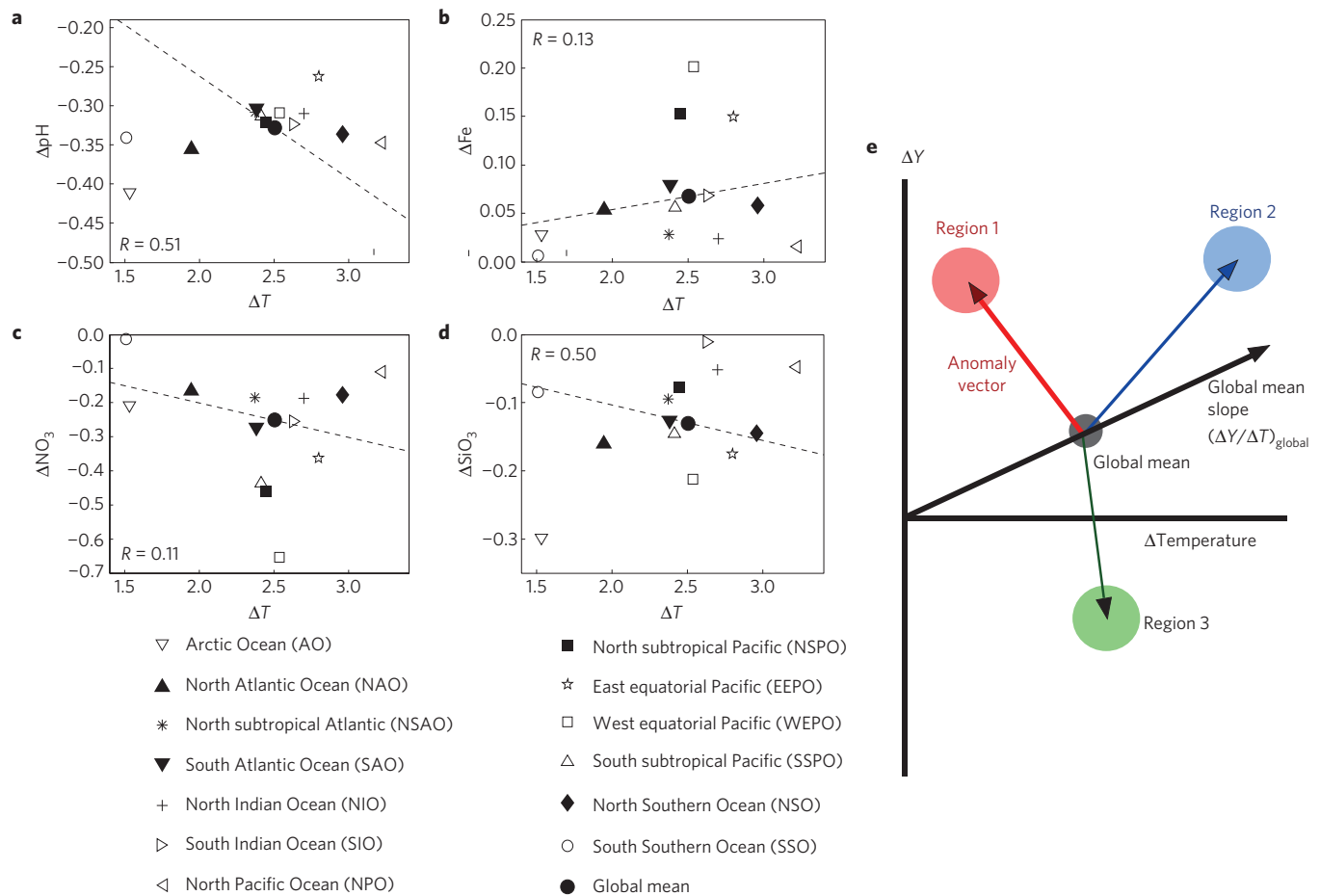
Figure 2 | Relationship between global and regional climate-driven trends in ocean properties. a–d, Regional variations in surface-ocean ΔpH (**a**), iron (ΔFe) (**b**), nitrate (ΔNO_3) (**c**) and silicate (ΔSiO_3) (**d**) as a function of the change in SST (ΔT). **e**, The temporal anomaly for any variable Y, ΔY, is computed from the model output as the future projection value (mean of 2081–2100) minus present (mean 1981–2000). The dashed lines in **a–d** and the black arrow in **e** show the linear regression (passing through the origin) of the global mean changes. As illustrated in **e**, before the factor analysis the model output is standardized, which involves subtracting the global mean ΔY values for each property (Table 1). For variables where the climate change signal is strongly correlated with warming, the resulting anomaly vectors will be aligned with the global mean slope ($\Delta Y/\Delta T$), similar to Region 2 in the schematic, and the climate change signal in property Y can be scaled from the ΔT map. In contrast, for other variables, more distinct regional anomaly vectors will occur that do not fall along the mean slope, similar to Regions 1 and 3 in the schematic.

thresholds (relative to the global mean trends) are crossed for one or more environmental stressors (for example, sea surface temperature (SST), subsurface oxygen) in a future ocean[7].

Such global modelling studies have gone a step further, finding, for example, approximate linear relationships across models between the climate change anomalies in global mean SST and those for global pH or net primary production[7] (NPP). In contrast, nonlinear relationships are found for global SST and global ocean oxygen inventory, a measure of subsurface deoxygenation more closely related (anti-correlated) to ocean heat content anomalies, which continue to grow in time in climate change scenarios even after SSTs stabilize[7]. Global-scale analyses, however, do not fully capture important regional variations in the relationships among the suite of changing ocean environmental properties. This is evident from Fig. 1 where, for example, SST changes in the Arctic are small (relative to other provinces) but are amplified regionally for pH and silicate; spatial patterns even differ between the macronutrients silicate and nitrate (Fig. 1).

Recent advances in integrating the effects of such complex environmental change on marine biota have taken place—for example, the use of matrices of environmental change[10]—that may be useful for advancing global modelling approaches.

Here, we express climate change projections in a new manner, by further evaluating simulations using rotated factor analysis, to establish regional patterns of complex environmental change in multi-stressors across the global ocean. Such patterns can then be interpreted biologically by examining the sensitivity of regional taxa to multi-stressors. The influence of independent and interactive effects of regionally distinct multi-stressors on phytoplankton dynamics can then be explored by interpreting them using a compilation of the outcomes from laboratory/field multi-stressor manipulation studies[10].

Regionally distinct patterns of multi-stressors

The first objective of the study is to identify and summarize regional variations in the strengths and relationships of the climate change signals among a range of different physical and biogeochemical forcing factors (or stressors). The model analysis was conducted on climate change scenario output across 14 provinces (Supplementary Fig. 1) from the fully coupled Community Earth System Model[15,16] (CESM1(BEC), detailed in Methods and Supplementary Methods).

The climate-change-mediated alteration of individual upper-ocean properties can be assessed visually from conventional

Table 2 | Summary of the changes in ocean properties using the difference between future and present-day projections (from Fig. 1) globally and for each of the 14 CESM1(BEC) regions (Supplementary Fig. 2).

	Temp. (°C)	Physical variables						Biogeochemical variables				CO_2 system			
		Salinity (psu)	Ice fraction –	Log_{10} MLD (cm)	PAR (W m^{-2})	Windstress (dyn cm^{-2})	Pot. density (kg m^{-3})	Log_{10} SiO$_3$ (mmol m^{-3})	Log_{10} PO$_4$ (mmol m^{-3})	Log_{10} Fe (mmol m^{-3})	Log_{10} NO$_3$ (mmol m^{-3})	Alkalinity (meq m^{-3})	CO$_3^{2-}$ (µmol kg^{-1})	pH –	p_{CO_2} (ppmv)
Global mean	2.50	−0.10	−0.03	−0.02	0.43	0.00	−0.73	−0.13	−0.31	0.07	−0.25	−6.52	−82.5	−0.33	486
SSO	1.51	−0.30	−0.19	−0.03	3.67	0.18	−0.35	−0.08	−0.01	0.01	−0.01	−2.7	−51.3	−0.3	440
NSO	2.96	0.02	0.00	−0.03	0.69	−0.05	−0.62	−0.15	−0.21	0.06	−0.18	−4.1	−73.8	−0.3	493
SSPO	2.41	−0.02	0.00	−0.01	−1.15	0.01	−0.79	−0.15	−0.34	0.06	−0.44	−6.8	−96.2	−0.3	488
WEPO	2.53	−0.48	0.00	−0.03	−1.68	0.03	−1.23	−0.21	−0.47	0.20	−0.65	−9.1	−98.7	−0.3	482
EEPO	2.80	−0.16	0.00	−0.04	−2.91	−0.03	−1.02	−0.18	−0.26	0.15	−0.36	−7.2	−73.1	−0.3	447
NSPO	2.44	−0.17	0.00	0.00	−0.33	−0.01	−0.92	−0.08	−0.52	0.15	−0.46	−7.8	−96.6	−0.3	493
NPO	3.22	−0.45	0.00	−0.03	0.99	0.02	−0.94	−0.05	−0.22	0.02	−0.11	−7.3	−66.2	−0.3	491
SIO	2.62	−0.20	0.00	0.01	0.45	−0.01	−1.01	−0.01	−0.44	0.07	−0.25	−4.7	−96.1	−0.3	494
NIO	2.70	−0.19	0.00	0.00	−0.78	0.04	−1.05	−0.05	−0.37	0.02	−0.19	−7.8	−96.6	−0.3	483
SAO	2.38	0.08	0.00	−0.01	−0.91	−0.02	−0.70	−0.13	−0.46	0.03	−0.27	−6.9	−93.3	−0.3	482
NSAO	2.37	0.55	0.00	0.00	−0.93	−0.01	−0.35	−0.09	−0.47	0.03	−0.19	−5.18	−96.0	−0.3	494
NAO	1.94	−0.19	−0.04	−0.08	1.49	−0.06	−0.57	−0.16	−0.20	0.05	−0.16	−12.0	−81.9	−0.4	495
AO	1.51	−0.30	−0.19	−0.03	3.67	0.18	−0.35	−0.08	−0.01	0.01	−0.01	−16.3	−48.8	−0.3	440

Red arrows denote an increase, and blue arrows denote a decrease in an ocean property. The arrows are scaled according to the regional deviation from the global mean; larger arrows indicate a stronger regional anomaly relative to the global mean anomaly, and smaller arrows a weaker regional anomaly. Together, these regional deviations, across ocean properties, drive distinctive patterns in multi-stressors. The acronyms for the regions are defined in Fig. 2 and Supplementary Fig. 1.

Regional anomalies

Largest regional anomaly   Global mean   Smallest regional anomaly

two-dimensional maps of the difference (temporal anomaly) between the future and present-day projections (Fig. 1 and Supplementary Fig. 2). However, rather than focus on changes in model fields individually, the aim here is to explore how multiple properties change concurrently with one another. To begin to address the question of 'What does the pattern for climate change multi-stressors look like for the global ocean?' we used the data presented in Fig. 1 to provide insights into which properties 'change together' globally (Supplementary Fig. 3). Table 1 shows statistical analyses for each model variable including the global mean temporal anomaly (future–present), where log normalization is used for some variables. As in previous studies[4,7,9], the future upper ocean is projected, on average, to be warmer with lower nutrient concentrations and reduced pH.

The climate change signal for each variable is a combination of the global mean change and regional variation (Fig. 2). For example, relatively small annual-mean surface warming is projected for the Arctic and south Southern Ocean ($\Delta T \sim +1.5\,°C$) compared with the global mean ($\Delta T + 2.5\,°C$) or subpolar oceans ($\Delta T \sim +3\,°C$; Fig. 2a–d); ice-covered regions exhibit less warming during winter and an amplification in the seasonal SST cycle. The regional temporal anomalies are more uniform for other annual-mean properties such as the partial pressure of carbon dioxide ($\Delta p_{CO_2} \sim +490$ ppmv) and pH (ΔpH -0.30 to -0.35). The more uniform change in surface-ocean carbonate chemistry occurs because of the spatial homogeneity in forcing driven by rising atmospheric CO_2; the Arctic Ocean is an exception with large pH reductions because of sea-ice melt and lower surface alkalinity[17].

The magnitude of the regional variation in these properties is reflected in Table 1 by the relatively small coefficients of variation for p_{CO_2} (0.05) and pH (0.07) and a larger value for temperature (0.26), where the coefficient of variation is defined as the spatial standard deviation divided by the global mean for the temporal anomaly field. Ocean warming and acidification are primary factors driving, both directly and indirectly, changes in other upper-ocean variables. However, the regional variations often do not correspond with the expectation from the global trends. For example, the average log-normalized surface silicate declines globally ($\Delta SiO_3 < 0$) but the grid-point correlation of $\Delta T - \Delta SiO_3$ is positive (0.22; Table 1) indicating the opposite relationship (larger declines in silicate occur in polar regions with smaller temperature increases; Fig. 2d).

To better characterize the climate change relationships among upper-ocean variables, factor analysis was performed on the
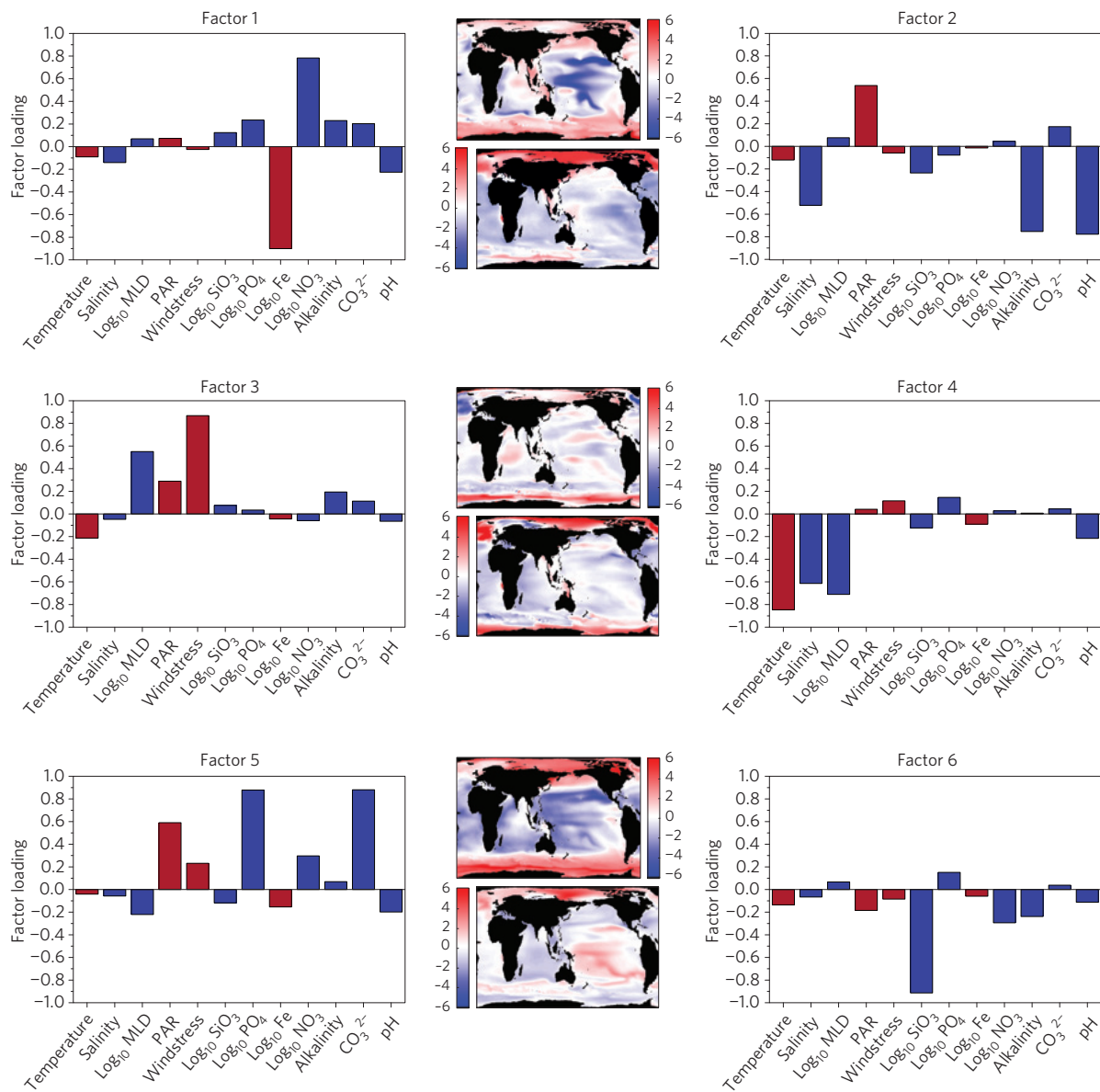
Figure 3 | Results of the factor analysis (Factors 1–6) based on data presented in Fig. 1 (two-dimensional global maps of the change in each ocean property between the decades 2081–2100 minus 1981–2000). For each factor, the bar plot shows the relationships among variables (factor loadings), where the colour coding indicates the sign of the global trend (red positive; blue negative). The maps between the bar plots indicate the spatial pattern (factor scores), and in each case the upper map of factor scores corresponds to the left panel factor loadings. The spatial patterns for any particular variable due to a particular factor can be recovered by multiplying the factor loading by the factor score map. In interpreting the factors, it is important to remember that they represent deviations from the global mean temporal anomalies (Fig. 2e). Thus, a negative factor loading (bar chart) and negative score (blue areas of the map) would result in a positive value (temporal anomaly greater than the global mean change) for that particular variable.

temporal anomaly fields (ΔT, ΔpH, and so on) on the original model grid ($\sim$1 degree horizontal resolution; Fig. 3). In interpreting the factors, it is important to consider that they represent deviations from the global mean temporal anomalies (Fig. 1); so, for example, in Factor 4 the large negative temperature values in the Arctic and Southern Ocean (negative factor loading shown in bar graph times positive factor scores in spatial map) reflect lower rates of warming than the global mean, rather than net cooling (global mean sign indicated by red colour of factor loading bar; Figs 1a and 2, and Table 2). Groups of properties are conspicuous from the factor analysis. In Factor 1, log-normalized nitrate (NO_3) and iron (Fe) are anti-correlated with a spatial dipole pattern between the low latitudes (lower nitrate and higher iron trends than in the global mean) and high latitudes (reverse pattern of lower latitudes).

Owing to increased vertical stratification and reduced upward macronutrient supply, surface nitrate declines everywhere, with the largest proportional changes in the north subtropical and tropical Pacific (Figs 1c and 2c); in contrast, with fixed atmospheric iron inputs through dust deposition and lower biological production, surface iron increases correspondingly.

The spatial patterns of the factor scores are often correlated (for example, the large-amplitude Arctic signals in Factors 2, 4 and 5; Supplementary Table 3). To assess the cumulative impact, regional departures from the global trends were computed for each oceanic province (Table 2), and a subset of four of the most conspicuous regional variations, relative to the global trends, is presented in Fig. 2a–d. There are pronounced regional departures from the global trends for both low-latitude and high-latitude provinces,

Table 3 | Ramifications of regional changes in climate change properties (year 2100) for phytoplankton in two illustrative high-latitude provinces (NSO and NAO).

High-latitude provinces (NSO; NAO)	Temp. (2.96 °C; 1.94 °C) ⬆	CO₂ (143%; 151%) ⬆	PAR (1%; 3%) ⬆	Iron (11%; 8%) ⬆	Silicate (32%; 29%) ⬇	NO₃ (18%; 30%) ⬇	PO₄ (21%; 31%) ⬇
Coccolithophores							
Effects of individual stressors	Warming enhances growth rates by ~25% (NAO; ref. 44)	Alters calcification (0−20% decrease, NSO; ref. 45)	–	Increased growth rate (17%; NAO; ref. 30)	–	–	Low PO₄ favours coccolithophores (NAO; ref. 31)
Effects of interactive stressors	Warming and high CO_2 cause a 40% decrease in calcification, but increase coccolithophore stocks (NAO; ref. 22)	Interactions with warming[22] (see left), and high PAR (ref. 31; see right)	High PAR and high CO_2 decrease calcification (NAO; ref. 31)	–	–	–	–
Diatoms							
Effects of individual stressors	Warming enhances growth by 35% (20); warming decreases cellular P requirements[46]	High CO_2 favours some diatom species and enhances NPP (ref. 32)	–	Enhances growth (NSO; ref. 47); Decreases silicification[21]	Decreases silicification[48]	–	–
Effects of interactive stressors	Warming and iron supply cause 400% enhancement of growth rates[14]	–	Higher PAR and iron jointly cause 200% increase in growth[49] (NAO)	Interactions with PAR (ref. 49; see left), and PAR and silicate (see right)	Iron, PAR and silicate interact to control summer diatom growth rates[47] (NSO)	–	Warming decreases cellular P requirements[46]
Coccolithophore versus diatom biogeography	Warming causes polewards shifts in coccolithophores[50] (NSO, NAO)	–	High PAR and low PO₄ favour coccolithophores[31] (NAO)	–	Shift to coccolithophores if silicate decreases to <2 µmol l⁻¹ (NSO; ref. 24)	–	Interacts with PAR (ref. 31; see left)

The change in each biologically influential property is expressed as a % (future minus present day, see Supplementary Table 1) except for temperature (warming in °C). The biological consequences are examined using a compilation of available laboratory/field manipulation studies and field surveys for the main phytoplankton groups in these waters—diatoms and coccolithophores. See Supplementary Table 4 for a parallel comparison in two illustrative low-latitude provinces. Red and blue arrows denote increases or decreases in climate change environmental properties. Blank cells denote no available data. PAR denotes mean underwater irradiance for the upper 10 m (averaged over 24 h for each month[16,42]). Note, the magnitude of the experimental manipulations presented here closely correspond to those projected by models for temperature and CO_2, whereas iron or nutrient manipulations often exceed model-predicted changes for 2100.

for example, in increased surface Fe concentration for the north subtropical Pacific Ocean (NSPO) and west and east equatorial Pacific (WEPO and EEPO). Such regional departures for these provinces were also evident for nitrate, silicate, temperature and phosphate (see also Table 2). The magnitudes of these departures are expressed as both percentage changes (Supplementary Table 1) and stoichiometric shifts (Supplementary Table 2). Together, these Figures, Tables and the factor analysis reveal the presence of regionally distinctive multi-stressor patterns that result from the integration of changes (that is, future minus present day) in the CESM1(BEC) model physics, chemistry and biology (Table 1 and Supplementary Tables 1 and 2 and Fig. 2).

Phytoplankton responses to multi-stressors

Changes to the properties within each region will exert both individual and multiple (independent versus interactive)[11,13] stresses that together will result in cumulative physiological[10,11] and/or biogeographical[4,18] effects on phytoplankton. Assessment of the effects of these regionally distinctive multi-stressor patterns (Table 2) on phytoplankton requires information on the composition of the resident phytoplankton in each province, along with data sets on the range of responses to environmental forcing by each major phytoplankton group from manipulation experiments[10] and/or time-series/survey observations[19] (Table 3 and Supplementary Table 4). Such an analysis enables the model data to be transformed into a preliminary appraisal of the effects of complex environmental change on the dominant phytoplankton groups within provinces (Supplementary Fig. 4). Our approach provides insights into the nature (independent versus interactive effects) and degree (that is, amplification versus diminution) of future changes to phytoplankton processes to be expected. In doing

so, it reveals many of the challenges that lie ahead for both the experimental manipulation and modelling communities as they attempt to better address oceanic multi-stressors.

An evaluation of how multi-stressors will influence phytoplankton reveals many responses that we do not fully understand (that is, beyond model parameterization at present[7–9]). They encompass altered physiological rates[20], compensatory effects between individual stressors[21], pronounced interactive effects[14,22,23], the likelihood of shifts in biomes[24–26], and the interplay of all of these responses to biologically restructure each province. Further regional distinctions are provided by information on differential responses to alteration of individual properties, such as the CO_2 affinities of nitrogen fixers from different provinces[27], or multi-stressors including the regional-specific response to altered Fe supply and irradiance evident for polar diatoms[28]. The stoichiometry of nutrient supply, as expressed by metrics such as P* (that is, P minus (N/16); ref. 29), also provides insights into how nutrient multi-stressors may influence future spatial patterns of the dominance of phytoplankton groups[19,26].

The widespread effects of regionally distinctive multi-stressors on resident phytoplankton, based on reports from laboratory studies and field surveys, have been compiled for two high-latitude provinces (Table 3). These provinces were highlighted as each is characterized by marked departures from global trends (Fig. 2), resulting in clear evidence of distinct multi-stressor regimes in the coming decades (Table 1 and Supplementary Tables 2 and 3). The northern Southern Ocean (NSO, see Supplementary Fig. 1) comprises a major biogeochemical feature—the Great Calcite Belt—reported to cover 16% of the global ocean[24]; thus, we have focused on how multi-stressor patterns projected for the NSO may alter coccolithophore and diatom dynamics (Table 3).

The NSO and northern Atlantic Ocean (NAO) coccolithophores will be subject to complex effects of multi-stressors ranging from individual (increased Fe supply increases growth rate (NAO); ref. 30), interactive (warming and higher CO_2 alters calcification and coccolithophore stocks (NAO); ref. 22), and a potential increase in their biome if a decrease in silicate, projected for the NSO, crosses the putative threshold between diatom ($>2\,\mu mol\,l^{-1}$) and coccolithophore dominance[24] (Table 3). In these provinces phosphate is projected to decline, potentially favouring coccolithophores[31]. The blank cells in Table 3 reveal that many unknowns also exist for coccolithophores, such as the interplay of Fe, temperature and CO_2, which each influence their physiology[22,30].

The NSO and NAO multi-stressor patterns will have similarly complex effects on diatoms (Table 3). The projected warming, enhanced Fe and decreased silicate supply each have a range of both individual and interactive effects. For example, warming will enhance growth[20], and increased Fe supply will probably offset the effects of decreased silicate supply by reducing the diatoms' silicate requirements[21]. Other potential interactive effects on NSO diatoms are based on evidence from south Southern Ocean (SSO) studies of warming and higher Fe supply synergistically increasing diatom growth rates[14], and of enhanced NPP and floristic shifts driven by higher CO_2 concentrations[32]. These experimental outcomes point to the likelihood of additional (but as yet unidentified) interactive effects on diatoms across all multi-stressors within high-latitude provinces. Hence, in our appraisal, prediction of the biological, ecological or biogeochemical outcomes of such complex climate change is not yet possible, but should be an overarching goal for the ocean science community.

A similarly complicated combination of individual and interactive effects of multi-stressors is evident for low-latitude provinces such as the South Atlantic Ocean (SAO, Supplementary Table 4). In this province, projected concurrent increases in Fe and decreases in both nitrate and phosphate supply will probably favour nitrogen fixers, as the SAO is characterized by P* of ∼0.3 at present[19,29]. Changes to other multi-stressors evident for the SAO such as warming and higher CO_2 will probably reinforce—both individually and interactively—the effects of alteration to Fe, NO_3 and PO_4 supply in increasing the areal extent of the nitrogen fixer biome[18,26] (within this province): higher CO_2 is reported to increase rates of nitrogen fixation[27] and warming may increase maximum potential growth rates by ∼25% (Supplementary Table 4).

The influence of multi-stressors on other dominant groups—*Prochlorococcus* and *Synechococcus*—in the SAO (refs 23,25) is less certain (Supplementary Table 4). For example, warming and reduced NO_3 may increase the geographic extent and hence size of the *Prochlorococcus* biome within this province[25,33]. However, such floristic shifts may be confounded by the 300% increase in maximum photosynthetic rates due to the synergistic effects of warming and higher CO_2 on *Synechococcus* compared with *Prochlorococcus*, which had a negligible photosynthetic response[23]. Although increased Fe supply has pronounced positive, but transient, effects on the physiology of both of these picoplanktonic groups during mesoscale experiments[34], its effect on resident SAO cells is largely unknown, as are any further interactive effects between Fe, NO_3, CO_2 and/or temperature. Many of these complex consequences of climate change on the resident NSPO phytoplankton are similar to those identified for the NSO. However, there is already evidence of some regional nuances, for example, the different CO_2 affinities of the nitrogen fixers in each province[27], which suggests that CO_2-mediated enhancement of nitrogen fixation will have a more pronounced effect by 2090–2099 in the SAO than in the NSPO.

This coupled Earth system model experiment and subsequent factor analysis have revealed that a significant number of oceanic provinces will encounter complex environmental change that differs significantly from that occurring globally. Such distinctive patterns in multi-stressors provide a potent linkage, regionally, between the output of model simulations and the likely physiological and biogeographical consequences for the phytoplankton within each province. As a result of this regional specificity, the resident groups and their distinctive responses to environmental forcing, a regional as opposed to a global approach is needed to advance this research field. Knowledge of the ecological[35] and biogeochemical[36,37] roles of these phytoplankton groups will provide further links between such environmentally modulated physiological consequences and the wider ecological and biogeochemical ramifications of a changing ocean.

So far, coupled Earth system models have largely been used to determine the effects of changing individual ocean properties (for example, temperature, light or nutrients) on bulk biological processes such as NPP (ref. 7). In common with many of the CMIP5 models, the CESM1(BEC) ocean biogeochemistry module includes only a subset of the potential multiplicative, synergistic and antagonistic effects of multi-stressors on planktonic ecosystems (Table 3 and Supplementary Table 4). For example, the model explicitly incorporates an interlinked treatment of variations in temperature, multiple nutrients and light on phytoplankton growth following the conceptual framework of ref. 38 as well as the effects of competition and selection of phytoplankton functional types driven by differential growth and zooplankton grazing[39]. The additional effects of stressors such as temperature, nutrients and light on phytoplankton diversity[9], or pH/CO_2 on phytoplankton growth, calcification and plankton elemental stoichiometry have been incorporated into specific model experiments[40,41] but are not universal across the present generation of coupled Earth system models, including CESM1(BEC).

The approach detailed here enables regions of complex climate change to be readily identified, and an initial appraisal of the subsequent effects of both individual and interactive effects of multi-stressors on phytoplankton groups to be carried out. It reveals gaps in our knowledge of phytoplankton responses to multi-stressors. Hence, it provides insights and new directions to both the oceanographic modelling and environmental manipulation communities about how to transition from representation of individual to multiple to interactive oceanic properties and their cumulative effects on ocean biota.

Methods

The CESM1(BEC) marine ecosystem module (BEC, Biogeochemistry/Ecosystem/Circulation) includes NPP and the explicit representation of three phytoplankton functional types (PFT)—diatoms, diazotrophs and small phytoplankton[42]. Model evaluation studies indicate that the CESM1(BEC) exhibits comparable skill against observations of present-day ocean physical and biogeochemical metrics and similar patterns of climate change to other CMIP5 Earth system models[7]. The discussion (in the main text) of the ramifications of the phytoplankton responses to multiple stressors (both individual and interactive effects) is focused only on a compilation of laboratory and field evidence, as opposed to the CESM1(BEC) model outputs for each PFT, as the PFTs as parameterized do not, as of yet, take into account the individual biological influence of each of the altered stressors (for example, the effects of increased CO_2 on diazotrophs[27]), nor their fully interactive effects[10,11] (with some exceptions such as interlinked temperature, nutrient and light effects on phytoplankton growth[38]).

As with all plankton functional type models, the CESM1(BEC) ecosystem model contains a number of assumptions regarding the biological responses of phytoplankton and zooplankton to environmental conditions (for example, temperature, nutrient and light response functions on photosynthesis and growth; elemental stoichiometry of biomass and detritus; rate functions for growth and mortality)[38,39]. The CESM(BEC) model is broadly similar in construction to other PFT models, although specific aspects of the climate change solutions will of course reflect the choices in functional form and parameters.

Two model time periods are used for comparison: the present day (1981–2000) and a future projection (2081–2100) following a high-emission

climate change scenario (RCP8.5) with a rapid rise in atmospheric CO_2. Spatial maps of 15 ocean variables are computed for both present and future conditions by averaging over 20-year periods to reduce the effect of interannual variability; difference maps (ΔT, ΔpH and so on) are then calculated by subtracting the future minus the present. Statistical and factor analysis, summarized in Supplementary Fig. 3, are conducted on the original model grid (~1 degree horizontal resolution). Regional binned products are also produced for illustrative purposes by averaging the model output into 14 standard provinces that approximately match large-scale ocean physical and biogeochemical boundaries (for example, subpolar upwelling versus subtropical downwelling gyres; Supplementary Fig. 1).

Factor analysis was performed on the temporal anomaly fields (ΔT, ΔpH and so on) on the original model grid (~1 degree horizontal resolution; Fig. 3). Twelve variables, chosen as a subset of the ocean variable fields, were standardized by removing the spatial mean and dividing by the spatial standard deviation (Supplementary Fig. 3 and Methods). Factor loadings (contributions of different upper-ocean variables to each factor) and factor scores (spatial patterns for each factor) were computed using singular value decomposition of the standardized variable covariance matrix[43]. On the basis of the communalities (a measure of variable representation, by factor), the 6 factors with the highest corresponding eigenvalues were kept for varimax rotation[43] and the resulting rotated factor loadings and scores are presented in Fig. 3. The spatial patterns for any particular standardized variable due to an individual factor can be recovered by multiplying the factor loading by the factor score map. The factor analysis helps visualize the multi-stressor patterns and characterize the main relationships among the stressor variables that contribute to these patterns. The major aspects of the regionally distinctive multi-stressor patterns can be reconstructed compactly at the model grid scale using the spatial patterns of the leading factors that explain the largest fraction of the global variance in the stressor variables.

References

1. Doney, S. C. The growing human footprint on coastal and open-ocean biogeochemistry. *Science* **328**, 1512–1516 (2010).
2. Gruber, N. Warming up, turning sour, losing breath: Ocean biogeochemistry under global change. *Phil. Trans. R. Soc. A* **369**, 1980–1996 (2011).
3. IPCC *Climate Change 2013: The Physical Science Basis* (eds Stocker, T. F. *et al.*) (Cambridge Univ. Press, 2013).
4. Sarmiento, J. L. *et al.* Response of ocean ecosystems to climate warming. *Glob. Biogeochem. Cycles* **18**, GB3003 (2004).
5. Riebesell, U. & Tortell, P. in *Ocean Acidification* (eds Gattuso, J-P. & Hansson, L.) 99–116 (Oxford Univ. Press, 2011).
6. Orr, J. C. *et al.* Anthropogenic ocean acidification over the twenty-first century and its impact on calcifying organisms. *Nature* **437**, 681–686 (2005).
7. Bopp, L. *et al.* Multiple stressors of ocean ecosystems in the 21st century: Projections with CMIP5 models. *Biogeosciences* **10**, 6225–6245 (2013).
8. Hood, R. R. *et al.* Pelagic functional group modeling: Progress, challenges and prospects. *Deep-Sea Res. II* **53**, 459–512 (2006).
9. Dutkiewicz, S., Scott, J. R. & Follows, M. J. Winners and losers: Ecological and biogeochemical changes in a warming ocean. *Glob. Biogeochem. Cycles* **27**, 463–477 (2013).
10. Boyd, P. W., Strzepek, R., Fu, F. X. & Hutchins, D. A. Environmental control of open-ocean phytoplankton groups: Now and in the future. *Limnol. Oceanogr.* **55**, 1353–1376 (2010).
11. Boyd, P. W. & Hutchins, D. A. Understanding the responses of ocean biota to a complex matrix of cumulative anthropogenic change. *Mar. Ecol. Prog. Ser.* **470**, 125–135 (2012).
12. Edwards, M., Reid, P. C. & Planque, B. Long-term and regional variability of phytoplankton biomass in the Northeast Atlantic (1960–1995). *ICES J. Mar. Sci.* **58**, 39–49 (2001).
13. Folt, C. L., Chen, C. Y., Moore, M. V. & Burnaford, J. Synergism and antagonism among multiple stressors. *Limnol. Oceanogr.* **44**, 864–877 (1999).
14. Rose, J. M. *et al.* Synergistic effects of iron and temperature on Antarctic phytoplankton and microzooplankton assemblages. *Biogeosciences* **6**, 3131–3147 (2009).
15. Hurrell, J. W. *et al.* The Community Earth System Model: A framework for collaborative research. *Bull. Am. Meteorol. Soc.* **94**, 1339–1360 (2013).
16. Moore, J. K., Lindsay, K., Doney, S. C., Long, M. C. & Misumi, K. Marine ecosystem dynamics and biogeochemical cycling in the Community Earth System Model CESM1(BGC). *J. Clim.* **26**, 9291–9321 (2013).
17. Steinacher, M., Joos, F., Frölicher, T. L., Plattner, G-K. & Doney, S. C. Imminent ocean acidification in the Arctic projected with the NCAR global coupled carbon cycle-climate model. *Biogeosciences* **6**, 515–533 (2009).
18. Boyd, P. W. & Doney, S. C. Modelling regional responses by marine pelagic ecosystems to global climate change. *Geophys. Res. Lett.* **29**, 531–534 (2002).
19. Moore, C. M. *et al.* Large-scale distribution of Atlantic nitrogen fixation controlled by iron availability. *Nature Geosci.* **2**, 867–871 (2009).
20. Boyd, P. W. *et al.* Marine phytoplankton temperature versus growth responses from polar to tropical waters—Outcome of a scientific community-wide study. *PLoS ONE* **8**, e63091 (2013).
21. Hutchins, D. A. & Bruland, K. W. Iron-limited diatom growth and Si:N uptake ratios in a coastal upwelling regime. *Nature* **393**, 561–564 (1998).
22. Feng, Y. *et al.* Effects of increased p_{CO_2} and temperature on the North Atlantic spring bloom. I. The phytoplankton community and biogeochemical response. *Mar. Ecol. Prog. Ser.* **388**, 13–25 (2009).
23. Fu, F-X., Warner, M. E., Zhang, Y., Feng, Y. & Hutchins, D. A. Effects of increased temperature and CO_2 on photosynthesis, growth, and elemental ratios in marine *Synechococcus* and *Prochlorococcus* (Cyanobacteria). *J. Phycol.* **43**, 485–496 (2007).
24. Balch, W. M. *et al.* The contribution of coccolithophores to the optical and inorganic carbon budgets during the Southern Ocean Gas Experiment: New evidence in support of the "Great Calcite Belt" hypothesis. *J. Geophys. Res.* **116** (Special Issue, C00F06), 1–14 (2011).
25. Johnson, Z. I. *et al.* Niche partitioning among Prochlorococcus ecotypes along ocean-scale environmental gradients. *Science* **311**, 1737–1740 (2006).
26. Ward, B. A., Dutkiewicz, S., Moore, C. M. & Follows, M. J. Iron, phosphorus, and nitrogen supply ratios define the biogeography of nitrogen fixation. *Limnol. Oceanogr.* **58**, 2059–2075 (2013).
27. Hutchins, D. A., Fu, F-X., Webb, E. A., Walworth, N. & Tagliabue, A. Taxon-specific response of marine nitrogen fixers to elevated carbon dioxide concentrations. *Nature Geosci.* **6**, 790–795 (2013).
28. Strzepek, R. F., Hunter, K. A., Frew, R. D., Harrison, P. J. & Boyd, P. W. Iron–light interactions differ in Southern Ocean phytoplankton. *Limnol. Oceanogr.* **57**, 1182–1200 (2012).
29. Deutsch, C., Sarmiento, J. L., Sigman, D. M., Gruber, N. & Dunne, J. P. Spatial coupling of nitrogen inputs and losses in the ocean. *Nature* **445**, 163–167 (2007).
30. Nielsdóttir, M. C., Moore, C. M., Sanders, R., Hinz, D. J. & Achterberg, E. P. Iron limitation of the postbloom phytoplankton communities in the Iceland Basin. *Glob. Biogeochem. Cycles* **23**, GB3001 (2009).
31. Zondervan, I. The effects of light, macronutrients, trace metals and CO_2 on the production of calcium carbonate and organic carbon in coccolithophores—a review. *Deep-Sea Res. II* **54**, 521–537 (2007).
32. Tortell, P. D. *et al.* CO_2 sensitivity of Southern Ocean phytoplankton. *Geophys. Res. Lett.* **35**, L04605 (2008).
33. Flombaum, P. *et al.* Present and future global distributions of the marine Cyanobacteria *Prochlorococcus* and *Synechococcus*. *Proc. Natl Acad. Sci. USA* **110**, 9824–9829 (2013).
34. Boyd, P. W. *et al.* Mesoscale iron enrichment experiments 1993–2005: Synthesis and future directions. *Science* **315**, 612–617 (2007).
35. Mulholland, M. R. The fate of nitrogen fixed by diazotrophs in the ocean. *Biogeosciences* **4**, 37–51 (2007).
36. Hutchins, D. A., Mulholland, M. R. & Fu, F-X. Nutrient cycles and marine microbes in a CO_2-enriched ocean. *Oceanography* **22**, 128–145 (2009).
37. Thomalla, S. J. *et al.* Variable export fluxes and efficiencies for calcite, opal, and organic carbon in the Atlantic Ocean: A ballast effect in action? *Glob. Biogeochem. Cycles* **22**, GB1010 (2008).
38. Geider, R. J., MacIntyre, H. L. & Kana, T. M. A dynamic regulatory model of phytoplanktonic acclimation to light, nutrients, and temperature. *Limnol. Oceanogr.* **43**, 679–694 (1998).
39. Marinov, I. *et al.* North–south asymmetry in the modeled phytoplankton response to climate change over the 21st century. *Glob. Biogeochem. Cycles* **27**, 1274–1290 (2013).
40. Oschlies, A., Schulz, K. G., Riebesell, U. & Schmittner, A. Simulated 21st century's increase in oceanic suboxia by CO_2-enhanced biotic carbon export. *Glob. Biogeochem. Cycles* **22**, GB4008 (2008).
41. Gehlen, M., Gruber, N., Gangstø, R., Bopp, L. & Oschlies, A. in *Ocean Acidification* (eds Gattuso, J-P. & Hansson, L.) Ch. 12, (Oxford Univ. Press, 2011).
42. Moore, J. K., Doney, S. C. & Lindsay, K. Upper ocean ecosystem dynamics and iron cycling in a global 3-D model. *Glob. Biogeochem. Cycles* **18**, GB4028 (2004).
43. Glover, D. M., Jenkins, W. J. & Doney, S. C. *Modeling Methods for Marine Science* 571 (Cambridge Univ. Press, 2011).
44. Conte, M. H., Thompson, A. T., Lesley, D. & Harris, R. P. Genetic and physiological influences on the alkenone/alkenoate versus growth temperature relationship in *Emiliania huxleyi* and *Gephyrocapsa oceanica*. *Geochim. Cosmochim. Acta* **62**, 51–68 (1998).
45. Langer, G. *et al.* Species-specific responses of calcifying algae to changing seawater carbonate chemistry. *Geochem. Geophys. Geosyst.* **7**, Q09006 (2006).

46. Toseland, A. *et al.* The impact of temperature on marine phytoplankton resource allocation and metabolism. *Nature Clim. Change* **3,** 979–984 (2013).

47. Boyd, P. W., LaRoche, J., Gall, M., Frew, R. & McKay, R. M. L. Role of iron, light, and silicate in controlling algal biomass in subantarctic waters SE of New Zealand. *J. Geophys. Res.* **104,** 13395–13408 (1999).

48. Martin-Jezequel, V. *et al.* Silicon metabolism in diatoms: Implications for growth. *J. Phycol.* **36,** 821–840 (2000).

49. Boyd, P. W. *et al.* Control of phytoplankton growth by iron supply and irradiance in the subantarctic Southern Ocean: Experimental results from the SAZ Project. *J. Geophys. Res.* **106,** 31573–31583 (2001).

50. Winter, A., Nendriks, J., Beaufort, L., Rickaby, R. E. M. & Brown, C. W. Poleward expansion of coccolithophores *Emiliania huxleyi. J. Plankton Res.* **36,** 316–325 (2013).

Acknowledgements

Author contributions

P.W.B. and S.C.D. designed the study; S.T.L. carried out the statistical analyses and provided the display items; D.M.G. carried out the statistical analysis; P.W.B. wrote the manuscript with contributions from S.C.D., S.T.L. and D.M.G.

Additional information

Supplementary information is available in the online version of the paper. Reprints and permissions information is available online at www.nature.com/reprints. Correspondence and requests for materials should be addressed to P.W.B.

Competing financial interests

The authors declare no competing financial interests.